

**AFRL-RX-TY-TR-2008-4522**



# **THE HYDROXYL RADICAL REACTION RATE CONSTANT AND PRODUCTS OF DIMETHYL SUCCINATE**

**Sheryl E. Calidonna and William R. Bradley**  
Applied Research Associates  
P.O. Box 40128  
Tyndall AFB, FL 32403

**Michael V. Henley and J. Raymond Wells**  
Air Force Research Laboratory

**MARCH 2008**

**Final Report for 15 December 1999 – 14 August 2007**

**DISTRIBUTION STATEMENT A: Approved for public release;  
distribution unlimited.**

**AIRBASE TECHNOLOGIES DIVISION  
MATERIALS AND MANUFACTURING DIRECTORATE  
AIR FORCE RESEARCH LABORATORY  
AIR FORCE MATERIEL COMMAND  
139 BARNES DRIVE, SUITE 2  
TYNDALL AIR FORCE BASE, FL 32403-5323**

## NOTICE AND SIGNATURE PAGE

Using Government drawings, specifications, or other data included in this document for any purpose other than Government procurement does not in any way obligate the U.S. Government. The fact that the Government formulated or supplied the drawings, specifications, or other data does not license the holder or any other person or corporation; or convey any rights or permission to manufacture, use, or sell any patented invention that may relate to them.

This report was cleared for public release by the Air Force Research Laboratory, Materials and Manufacturing Directorate, Airbase Technologies Division, Public Affairs and is available to the general public, including foreign nationals. Copies may be obtained from the Defense Technical Information Center (DTIC) (<http://www.dtic.mil>).

REPORT NUMBER AFRL-RX-TY-TR-2008-4522 HAS BEEN REVIEWED AND IS APPROVED FOR PUBLICATION IN ACCORDANCE WITH ASSIGNED DISTRIBUTION STATEMENT.

\_\_\_\_\_  
//signature//  
MICHAEL V. HENLEY  
Work Unit Manager

\_\_\_\_\_  
//signature//  
DANIEL M. SAUCER, Major, USAF  
Chief, Airbase Sciences Branch

\_\_\_\_\_  
//signature//  
ALBERT N. RHODES, Ph.D.  
Acting Chief, Airbase Technologies Division

This report is published in the interest of scientific and technical information exchange, and its publication does not constitute the Government's approval or disapproval of its ideas or findings.

<b>REPORT DOCUMENTATION PAGE</b>				<i>Form Approved OMB No. 0704-0188</i>	
<small>The public reporting burden for this collection of information is estimated to average 1 hour per response, including the time for reviewing instructions, searching existing data sources, gathering and maintaining the data needed, and completing and reviewing the collection of information. Send comments regarding this burden estimate or any other aspect of this collection of information, including suggestions for reducing the burden, to Department of Defense, Washington Headquarters Services, Directorate for Information Operations and Reports (0704-0188), 1215 Jefferson Davis Highway, Suite 1204, Arlington, VA 22202-4302. Respondents should be aware that notwithstanding any other provision of law, no person shall be subject to any penalty for failing to comply with a collection of information if it does not display a currently valid OMB control number.</small>					
<b>PLEASE DO NOT RETURN YOUR FORM TO THE ABOVE ADDRESS.</b>					
<b>1. REPORT DATE (DD-MM-YYYY)</b>		<b>2. REPORT TYPE</b>		<b>3. DATES COVERED (From - To)</b>	
<b>4. TITLE AND SUBTITLE</b>				<b>5a. CONTRACT NUMBER</b>	
				<b>5b. GRANT NUMBER</b>	
				<b>5c. PROGRAM ELEMENT NUMBER</b>	
<b>6. AUTHOR(S)</b>				<b>5d. PROJECT NUMBER</b>	
				<b>5e. TASK NUMBER</b>	
				<b>5f. WORK UNIT NUMBER</b>	
<b>7. PERFORMING ORGANIZATION NAME(S) AND ADDRESS(ES)</b>				<b>8. PERFORMING ORGANIZATION REPORT NUMBER</b>	
<b>9. SPONSORING/MONITORING AGENCY NAME(S) AND ADDRESS(ES)</b>				<b>10. SPONSOR/MONITOR'S ACRONYM(S)</b>	
				<b>11. SPONSOR/MONITOR'S REPORT NUMBER(S)</b>	
<b>12. DISTRIBUTION/AVAILABILITY STATEMENT</b>					
<b>13. SUPPLEMENTARY NOTES</b>					
<b>14. ABSTRACT</b>					
<b>15. SUBJECT TERMS</b>					
<b>16. SECURITY CLASSIFICATION OF:</b>			<b>17. LIMITATION OF ABSTRACT</b>	<b>18. NUMBER OF PAGES</b>	<b>19a. NAME OF RESPONSIBLE PERSON</b>
a. REPORT	b. ABSTRACT	c. THIS PAGE			<b>19b. TELEPHONE NUMBER (Include area code)</b>

(Continued from SF 298, Block 14.)

observed as a secondary product being formed at a rate of  $(4.6 \pm 1.3) \times 10^{14}$  molecules  $\text{second}^{-1}$ , 60 minutes after initiating the OH + DMS reaction. Formic acid is believed to be a degradation product of the primary product, methyl glyoxylate (MG,  $\text{CH}_3\text{OC}(=\text{O})\text{C}(=\text{O})\text{H}$ ). Product formation pathways are discussed in light of current understanding of the atmospheric chemistry of oxygenated organic compounds.

## PREFACE

This is the final report in a series of reports accomplished under this work unit. The report describes work conducted to determine the kinetics and products of the gas-phase hydroxyl radical reaction with dimethyl succinate. Additional reports and publications resulting from this work unit are not described herein but are listed below for reference.

Baxley, J. Steven and J.R. Wells, "The Hydroxyl Radical Rate Constant and Atmospheric Transformation of 2-Butanol and 2-Pentanol," AFRL-ML-TY-TP-2000-4509, Apr 1998, Air Force Research Laboratory, Airbase & Environmental Technology Division.

Henley, M.V., W.R. Bradley, S.E. Wyatt, G.M. Graziano and J.R. Wells, "Atmospheric Transformation of Volatile Organic Compounds," in *Chemical and Biological Sensing*, Patrick J. Gardner, Editor, Proceedings of SPIE Vol. 4036, 24-30 (2000).

Bradley, W.R., S.E. Wyatt, J.R. Wells, M.V. Henley and G.M. Graziano, "The Hydroxyl Radical Reaction Rate Constant and Products of Cyclohexanol," *Int. J. Chem. Kinet*, 33, 108-117 (2001).

Henley, M.V., R.M. Weber and S.E. Wyatt, "Evaluation of Volatile Organic Compound Emissions from High Explosive Formulations," AFRL-ML-TY-TR-2002-4534, May 2002, Air Force Research Laboratory, Air Expeditionary Forces Technologies Division.

Henley, M.V., G.M. Graziano, M.A. Kovalchek, R.M. Weber and S.E. Wyatt, "Atmospheric Chemistry of Acetoin," AFRL-ML-TY-TR-2002-4535, May 2002, Air Force Research Laboratory, Air Expeditionary Forces Technologies Division (limited document).

Henley, M.V. and R.M. Weber, "Evaluation of Volatile Organic Compound Emissions from Line-X XS-350 Polymer Coating," AFRL-ML-TY-TR-2002-4608, November 2002, Air Force Research Laboratory, Air base Technologies Division.

Henley, M.V., R.M. Weber and S.E. Wyatt, "Evaluation of Volatile Organic Compound Emissions from the Preparation and Application of BoeGel-EP II," AFRL-ML-TY-TR-2002-4609, November 2002, Air Force Research Laboratory, Air base Technologies Division.

Renard, J.J., S.E. Wyatt and M.V. Henley, "Fate of ammonia in the atmosphere—a review for applicability to hazardous releases," *Journal of Hazardous Materials*, 108: 1-2: 29-60, 2004.

Renard, J.J., S.E. Wyatt and M.V. Henley, "Fate of ammonia in the atmosphere—a review for applicability to hazardous releases," AFRL-ML-TY-TP-2003-4541, January 2004, Air Force Research Laboratory, Airbase Technologies Division (postprint *J Haz Mat.*, **2004**, 108, 29-60).

Henley, Mike, Sheryl Calidonna and Jean Renard, "Atmospheric Kinetics for Toxic Industrial Compounds (TICs)," AFRL-ML-TY-TP-2005-4563, Jun 2006, Air Force Research Laboratory, Airbase Technologies Division.

Bradley, W.R., S.E. Wyatt, J.R. Wells, M.V. Henley and G.M. Graziano, "The Hydroxyl Radical Reaction Rate Constant and Products of Cyclohexanol," AFRL-RX-TY-TP-2008-4525, Mar 2008, Air Force Research Laboratory, Airbase Technologies Division. (postprint *Int. J. Chem. Kinet*, **2001**, 33, 108).

Henley, M.V., W.R. Bradley, S.E. Wyatt, G.M. Graziano and J.R. Wells, "Atmospheric Transformation of Volatile Organic Compounds," AFRL-ML-TY-TP-2000-4529, Mar 2008, Air Force Research Laboratory, Airbase Technologies Division (postprint SPIE, **2000**, 4036, 24).

## SUMMARY

The objective of this report is to document the study of the gas-phase reaction of the hydroxyl radical (OH) with dimethyl succinate (DMS,  $\text{CH}_3\text{OC}(=\text{O})\text{CH}_2\text{CH}_2\text{C}(=\text{O})\text{OCH}_3$ ). With the increased usage of oxygenated organic compounds in paints and paint strippers as replacements for regulated volatile organic carbon containing-solvents and in fuels to promote better combustion, a better understanding of their environmental impact to the atmosphere is necessary. Previous studies of the products from OH + oxygenated organic reactions have illustrated the complexity of their atmospheric reaction mechanisms. Detailed studies of the reaction kinetics and products are needed to support hydroxyl radical reaction mechanism patterns based on structure-activity relationships (SAR) which are used to determine environmental impact.

The relative rate technique was used to examine the kinetics for the gas-phase reaction of OH + DMS. In these experiments the OH radical was generated from the photolysis of methyl nitrite in the presence of DMS, nitric oxide and a reference organic compound having a published rate constant for reaction with OH. The loss of DMS relative to the loss of the reference was used to determine the DMS rate constant. The measured rate constant was  $(1.5 \pm 0.4) \times 10^{-12} \text{ cm}^3 \text{ molecule}^{-1} \text{ s}^{-1}$  at  $297 \pm 3 \text{ }^\circ\text{K}$  and 1 atmosphere total pressure. This is in agreement with the predicted value of  $1.15 \times 10^{-12} \text{ cm}^3 \text{ molecule}^{-1} \text{ s}^{-1}$  determined by SAR.

To more clearly define DMS's atmospheric degradation mechanism, the products of the OH + DMS reaction were also investigated. The only primary product detected was mono methyl succinate (MMS,  $\text{CH}_3\text{OC}(=\text{O})\text{CH}_2\text{CH}_2\text{C}(=\text{O})\text{OH}$ ) at a yield of only

$2.17 \pm 0.25\%$ . Extensive efforts were used to identify other primary products but none were measured. Formic acid ( $\text{HC(=O)OH}$ ); however, was observed as a secondary product being formed at a rate of  $(4.6 \pm 1.3) \times 10^{14}$  molecules  $\text{second}^{-1}$ , 60 minutes after initiating the OH + DMS reaction. Formic acid is believed to be a degradation product of the primary product, methyl glyoxylate (MG,  $\text{CH}_3\text{OC(=O)C(=O)H}$ ). Product formation pathways are discussed in light of current understanding of the atmospheric chemistry of oxygenated organic compounds.



## TABLE OF CONTENTS

PREFACE .....	iii
SUMMARY .....	v
TABLE OF CONTENTS .....	vii
LIST OF FIGURES .....	viii
1.0 INTRODUCTION .....	1
2.0 EXPERIMENTAL METHODS .....	2
2.1 Apparatus and Materials .....	2
2.2 Experimental Procedures .....	6
3.0 RESULTS .....	8
3.1 OH + DMS Reaction Rate Constant .....	8
3.2 OH + DMS Reaction Products .....	9
3.3 <i>Mono Methyl Succinate (MMS, CH<sub>3</sub>OC(=O)CH<sub>2</sub>CH<sub>2</sub>C(=O)OH)</i> .....	11
3.4 <i>Formic Acid (FA, HOC(=O)H)</i> .....	15
3.5 <i>Nitrate/Nitrite Products</i> .....	15
4.0 DISCUSSION .....	17
<i>Acknowledgment</i> .....	20
5.0 REFERENCES .....	21

## LIST OF FIGURES

Figure 1. Dimethyl succinate reaction with methyl ethyl ketone and diethyl ketone.....	10
Figure 2. Plot of monomethyl succinate formed versus DMS reacted .....	12
Figure 3. Formic acid formation over time.....	16
Figure 4. Proposed reaction mechanism for hydroxyl radical with dimethyl succinate.....	20

## 1.0 INTRODUCTION

Oxygenated organic compounds are being used in paints and paint strippers as replacements for regulated VOC solvents. Oxygenated organics are also being used in fuels to promote better combustion, increase octane rating, reduce the production of carbon monoxide and reduce photochemically active volatile exhaust emissions. With the increased usage of these compounds, a better understanding of their environmental impact is necessary. While several hydroxyl radical (OH) + oxygenated organic bimolecular rate constants are well known, details pertaining to the reaction mechanisms are limited. The few completed studies of the products from OH + oxygenated organic reactions have illustrated the complexity of their atmospheric reaction mechanisms [1–5]. These details are needed to support hydroxyl radical reaction mechanism patterns based on structure–activity relationships (SAR) which are used to determine environmental impact [6].

The newly revised ozone (O<sub>3</sub>) and particulate matter regulations of the Clean Air Act Amendments have placed a greater emphasis on understanding detailed atmospheric mechanisms of oxygenated organic compounds. While not emitted directly, O<sub>3</sub> is a by-product of the photooxidation of volatile organic compounds [7]. Thus, sources that contribute to O<sub>3</sub> formation in the troposphere, either directly or indirectly, are or could be regulated. Currently, the reactivity models used to calculate a compound's incremental reactivity incorporate educated assumptions about a compound's unknown atmospheric mechanism [8]. In order to minimize uncertainties and calculate a compound's incremental reactivity more accurately, the rate constant and the transformation mechanism of that

compound must be well understood. This need has been demonstrated in a recent paper by Bergin *et al.* [9]

As a side benefit, understanding the compounds' atmospheric mechanisms in detail can provide a basis for chemical selection based on structure. There is the possibility of synthesizing new compounds that incorporate environmentally *and* technically beneficial molecular structures. The information gained from the type of research presented here can lead to more beneficial use of these and similar compounds in the future.

Dimethyl succinate (DMS,  $\text{CH}_3\text{OC}(=\text{O})\text{CH}_2\text{CH}_2\text{C}(=\text{O})\text{OCH}_3$ ) is one of a series of oxygenated organics present in consumer product formulations as a possible substitute solvent. In the work presented here, the rate constant of  $\text{OH} + \text{DMS}$  was measured by the relative rate method [10]. The products of the  $\text{OH} + \text{DMS}$  reaction are also reported and used to derive the DMS atmospheric reaction mechanism. The reaction mechanism for DMS has not been reported previously.

## 2.0 EXPERIMENTAL METHODS

### 2.1 Apparatus and Materials.

Experiments to measure the gas-phase rate constant and transformation products of the  $\text{OH} + \text{dimethyl succinate}$  (DMS,  $\text{CH}_3\text{OC}(=\text{O})\text{CH}_2\text{CH}_2\text{C}(=\text{O})\text{OCH}_3$ ) reaction were conducted with a previously described apparatus [1, 11,12]. A brief description is provided here. Reactants were introduced and samples were withdrawn through a 6.4-mm Swagelok fitting attached to a 100-L, 2-mil FEP Teflon<sup>®</sup>-film bag. The filler system was equipped with a syringe injection port facilitating the introduction of both liquid and gaseous

reactants into the bag by a flowing airstream. The syringe injection port was heated to insure DMS vaporization (200 °C boiling point). Dry compressed air was used as the diluent to the reaction bag and measured with a 0–100 L·min<sup>-1</sup> mass flow controller. All reactant mixtures and calibration standards were generated by this system. Irradiations were carried out in a light-tight chamber with the bag surrounded by the following mix of lamps: six Philips TL40W/03; one GE F40BL; two QPANEL UV351 and seven QPANEL UV340. This lamp mixture approximates solar radiation from 300 to 450 nm. The entire reaction chamber was maintained at 25 °C.

Kinetic experiments were quantitatively monitored using a Hewlett–Packard (HP) gas chromatograph (GC) 5890 with a flame ionization detector (GC/FID) or a mass selective detector (GC/MS) and HP series ChemStation™ software. Gas samples for both detectors were cryogenically collected on a Hastelloy C sample loop (1.3 mL) and injected onto the GC column (Restek Rtx-1 or Stabilwax column (0.53 mm i.d., 30 m, 1.0 µm film thickness)) with a heated rotary valve [13]. The GC/FID temperature program used was as follows: 35°C for 5 minutes then 10°C/min to 130°C and held for 5 minutes then 20°C/min to 200°C and held for one minute. The GC/MS temperature program used was as follows: 35°C for 5 minutes then 10°C/min to 255°C and held for one minute. Helium (UHP grade), the carrier gas, was supplied by Air Products and used as received.

Product identification experiments were accomplished with a HP 5890 Series II Plus GC/ HP 5971 mass selective detector/HP 5965B infrared detector (GC/MS/FTIR) system. The mass selective detector was tuned using perfluorotributylamine (FC-43). Full-scan electron impact ionization spectra were collected from 25 to 220 mass units. The infrared detector (GC/MS/FTIR) was operated at 8 cm<sup>-1</sup> resolution with four scans averaged to give

a single IR spectrum every 1.5 seconds. Preliminary compound identifications from the GC/MS/FTIR data sets were made by searching the Wiley/NBS Mass Spectra Library and the EPA vapor library. Pure samples of the identified products, if available, were then analyzed to check for matching spectra (MS and FTIR) and retention times. Compound separation was achieved using the same chromatographic parameters of the GC/MS as described above.

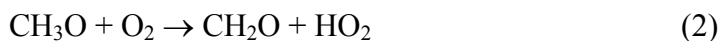
To determine carbonyl compounds produced by the gas-phase reaction of OH + DMS, 10 liters of chamber content were flowed over 2,4-dinitrophenylhydrazine (DNPH) impregnated cartridges. Hydrazones formed by derivatization were separated and quantitatively measured by HPLC (HP 1050) using a three-component gradient solvent program and UV detection as described previously [14].

Due to the very low number of products and their low yields for OH + DMS found using the instruments listed above, a ThermoQuest Trace 2000 Series GC in series with a GCQ Plus MS/MS, new to this laboratory, was implemented to try and identify fragments of product fragments. The MS/MS feature could lend insight to the primary products of OH + DMS that were not being seen by traditional methods. Gas samples from a 100-L Teflon® bag were collected cryogenically as described above. Approximately 1.3-mL samples were directly delivered to the mass spectrometer electron ionization (EI) source through a 0.18 mm ID x 5 m length of Restek Hydroguard FS guard column using the GCQ diffusion pump, which provided a vacuum of  $10^{-3}$  Pa ( $10^{-5}$  Torr). In the EI source, a beam of electrons, maintained at a negative potential of -70V relative to the ion volume, transferred the formed ions into the mass analyzer using three ion-focusing lenses.

Drawn by a DC offset voltage (-10V positive/+10V negative polarity mode) the ions entered the mass analyzer where a ring electrode between the endcaps was ramped from low to high voltage causing ions of greater mass-to-charge ratios to become unstable, thus creating collision induced dissociation. These product ions were ejected from the mass analyzer, through the exit lens, and focused toward the ion detection system. The ion detector used was a high-sensitivity, off-axis system that included a 15-kV conversion dynode and a continuous-dynode electron multiplier.

In all identification experiments, the GCQ was operated in the positive ion mode using both scanning (MS) and collision-induced dissociation (MS/MS) methods. For MS/MS experiments, the particles were ionized at >1 eV (determined during real-time) with a scan range of 35–250 *m/z*.

Hydroxyl radical, the primary oxidizing radical in the atmosphere, was generated from the photolysis of methyl nitrite (CH<sub>3</sub>ONO) in the presence of nitric oxide (NO) in air [10].



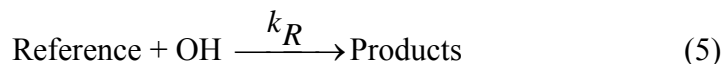
CH<sub>3</sub>ONO was prepared in gram quantities using the method of Taylor *et al.* [15] and stored in a lecture bottle at room temperature. The CH<sub>3</sub>ONO purity (>95%) was verified by GC/MS/FTIR.

All other compounds were used as received. Dimethyl succinate (99%) was purchased from Du Pont Chemicals. Chem Service supplied diethyl ketone (98%). Methyl ethyl ketone (99+%) and monomethyl succinate (95%) were received from Aldrich. Fisher

Scientific produced the methanol and acetonitrile (HPLC Grade). Water was distilled, deionized to 18 megaohm, and filtered using a Milli-Q® filter system. Dinitrophenylhydrazine (DNPH) standards were purchased from Radian Corporation. Nitric oxide (5000 ppm) was obtained from Matheson Gases. Experiments were carried out at  $297 \pm 3$  °K and atmospheric pressure.

## 2.2 Experimental Procedures

The experimental procedures for determining the OH + DMS reaction kinetics were similar to those described previously [11, 12].



The rate equations for reactions (4) and (5) are combined and integrated resulting in the following equation:

$$\ln \left( \frac{[\text{DMS}]_0}{[\text{DMS}]_t} \right) = \frac{k_{DMS}}{k_R} \ln \left( \frac{[\text{R}]_0}{[\text{R}]_t} \right) \quad \text{I}$$

If reaction with OH is the only removal mechanism for DMS and reference, a plot of  $\ln([\text{DMS}]_0/[\text{DMS}]_t)$  versus  $\ln([\text{R}]_0/[\text{R}]_t)$  yields a straight line with an intercept of zero. Multiplying the slope of this linear plot by  $k_R$  yields  $k_{DMS}$ . The OH rate constant experiments for DMS employed the use of two reference compounds, diethyl ketone (DEK) and methyl ethyl ketone (MEK). The use of two reference compounds with different OH rate constants, one faster and one slower than the expected rate constant for DMS, more definitively assured the accuracy of the OH + DMS rate constant and provided evidence that other reactions were not involved in DMS removal from the system.



For rate constant determination, the typical concentrations of the pertinent species in the 100-L Teflon<sup>®</sup> bag were 4.4 – 7.3 ppm DMS, 3.5–5.5 ppm reference, 40 ppm CH<sub>3</sub>ONO, and 2 ppm NO in air. The bag was sampled for initial species concentration ( $[X_0]$ ) and then irradiated for 45, 75, 105, and 135 seconds. These initial and irradiated mixtures were allowed to stand for 30–60 minutes before samples were collected on a cryogenic (-100 °C) sample loop (described above) for 4 minutes at 25 mL min<sup>-1</sup> and then flash injected (300 °C) onto the GC column [13]. The combined total photolysis time was approximately 360 seconds, which resulted in 30% loss of DMS, 35 % loss of DEK, and 20% loss of MEK. The flame ionization detector (FID) signal or total ion chromatogram (TIC) was used to quantify DMS and reference compound concentrations.

The technique for identification of OH + DMS reaction products was similar to the experimental methods and parameters for kinetic experiments except that the reference compound was excluded from the reaction mixture and the DMS concentration was approximately doubled (6.9–7.7 ppm). The irradiation intervals were the same as in the kinetic experiments so that total DMS loss was less than 50%. These conditions are favorable for ascertainment of products from OH attack at a single site on the DMS molecule. Excessive irradiation may lead to consecutive OH attack at several sites, which could result in false product identification. The mass selective detector (MS and MS/MS) and infrared detector (FTIR) were used for product determination.

All measurements were at least duplicated. A relative standard deviation (the data set standard deviation divided by the data set average) of approximately 2.5% was achieved with the described sampling method. Several interference experiments were conducted to assure the validity of the OH rate constant and product identification. They consisted of

looking for possible chromatographic co-elution of methyl nitrite, NO, reference, DMS and the hydroxyl radical reaction products. Two experiments were conducted to determine the stability of the reference and DMS co-existing in the same bag. First the reference and DMS were injected into the bag, quantified, photolyzed for 10 minutes and re-quantified. Second methyl nitrite, NO, reference and DMS were injected into the bag, quantified, left to sit overnight and then re-quantified. None of these preliminary experiments yielded chromatographic peak overlaps or observable reactions occurring without photoinitiation. The results showed that no significant wall interaction took place. At the end of each run, the Teflon<sup>®</sup> bag was cleaned by flushing six times with air containing <0.1 ppm total hydrocarbon. Measurements of an air-filled bag showed no cross contamination between runs.

### 3.0 RESULTS

#### 3.1 OH + DMS Reaction Rate Constant

The OH rate constant for dimethyl succinate (DMS,  $\text{CH}_3\text{OC}(=\text{O})\text{CH}_2\text{CH}_2\text{C}(=\text{O})\text{OCH}_3$ ) was obtained using the relative rate method described above. Typically five experimental runs were conducted on each DMS/reference pair. The plot of a modified version of equation I is shown in Figure 1. The  $\ln([R]_0/[R]_t)$  term is divided by the respective reference rate constant (methyl ethyl ketone (MEK)  $(1.15 \pm 0.29) \times 10^{-12} \text{ cm}^3 \text{ molecule}^{-1} \text{ s}^{-1}$  and diethyl ketone (DEK)  $(2.0 \pm 0.5) \times 10^{-12} \text{ cm}^3 \text{ molecule}^{-1} \text{ s}^{-1}$ ) [16] and multiplied by  $10^{-12} \text{ cm}^3 \text{ molecule}^{-1} \text{ s}^{-1}$  resulting in a unitless number. This yields a slope that is equal to the OH + DMS rate constant,  $k_{\text{DMS}}$ , divided by  $10^{-12} \text{ cm}^3 \text{ molecule}^{-1} \text{ s}^{-1}$ . This modification allows for a direct comparison of the two reference compound/DMS data

sets. The slope of combined data, as shown in Figure 1, results in a hydroxyl radical bimolecular rate constant,  $k_{DMS}$ , of  $(1.46 \pm 0.04) \times 10^{-12} \text{ cm}^3 \text{ molecule}^{-1} \text{ s}^{-1}$ . The data points at the origin are experimental points because pre-irradiation,  $t = 0$ , data showed no detectable loss of DMS or reference. The error in the rate constant stated above is the 95% confidence level from the random uncertainty in the slope. Incorporating the uncertainties associated with the reference rate constants ( $\pm 25\%$ ) used to derive the OH + DMS rate constant yields a final value for  $k_{DMS}$  of  $(1.5 \pm 0.4) \times 10^{-12} \text{ cm}^3 \text{ molecule}^{-1} \text{ s}^{-1}$ . Assuming an  $[\text{OH}] = 1 \times 10^6 \text{ molecules cm}^{-3}$ , the atmospheric (1/e) lifetime calculated for DMS is 190 hours. The observed OH + DMS rate constant is in excellent agreement with previously measured  $k_{DMS} = 1.4 \pm 0.6 \times 10^{-12} \text{ cm}^3 \text{ molecule}^{-1} \text{ s}^{-1}$  [17], and with  $k_{DMS} = 1.15 \times 10^{-12} \text{ cm}^3 \text{ molecule}^{-1} \text{ s}^{-1}$  calculated using structure–activity relationships (SAR) [18].

### **3.2 OH + DMS Reaction Products**

The reaction products observed from the initial OH + DMS hydrogen abstraction are consistent with previously observed hydroxyl radical reaction mechanisms for oxygenated organic species [1–4]. Typically, the oxygenated organic parent compound reacts with OH to subsequently generate other oxygenated organic products. For DMS, the OH + DMS reaction products observed were: monomethyl succinate (MMS,  $\text{CH}_3\text{OC}(=\text{O})\text{CH}_2\text{CH}_2\text{C}(=\text{O})\text{OH}$ ) and a secondary product, formic acid (FA,  $\text{HOC}(=\text{O})\text{H}$ ). The specific results for each of these products are described below.

Typically, the loss of the parent compound is plotted against the formation of products generating a straight line with a slope equal to the product yield. However, because

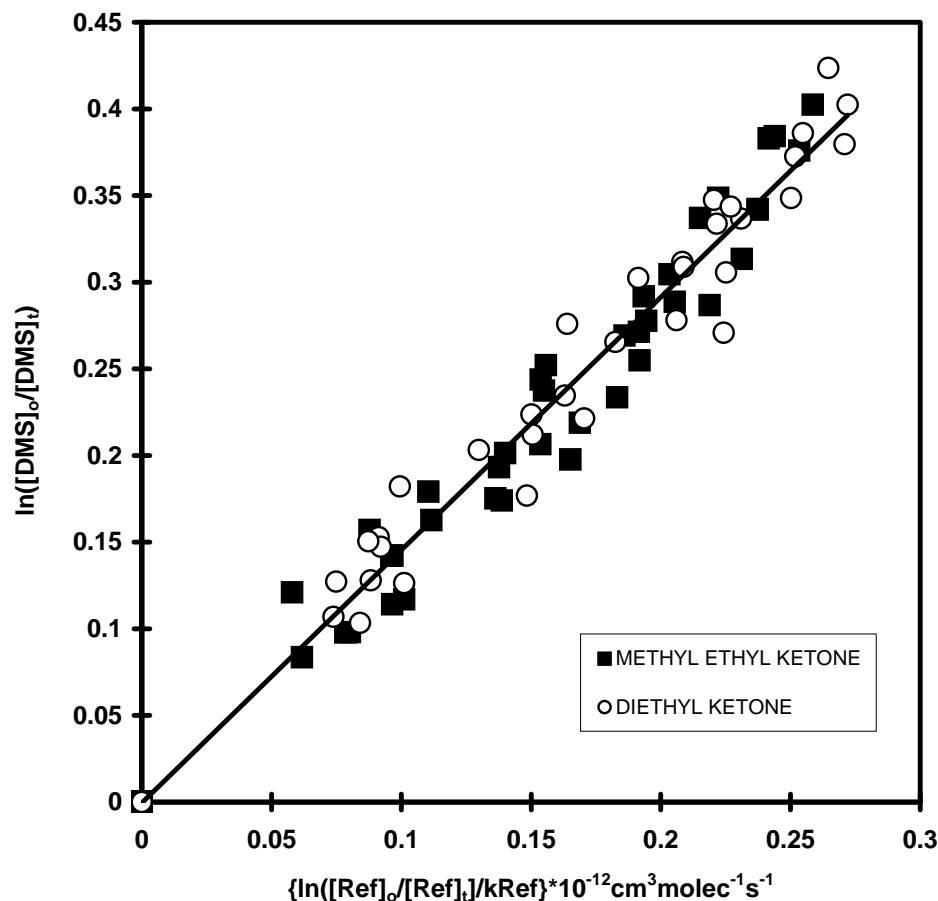


**Figure 1. Dimethyl succinate reaction with methyl ethyl ketone and diethyl ketone.** Dimethyl succinate relative rate plot with methyl ethyl ketone ( $\blacksquare$ ), and diethyl ketone ( $\circ$ ) as reference compounds. The OH + DMS rate constant,  $k_{DMS}$ , measured is  $1.46 \pm 0.04 \times 10^{-12} \text{ cm}^3 \text{ molecule}^{-1} \text{ s}^{-1}$ .

the OH + DMS reaction products could react with OH, the observed product concentrations have to be corrected for OH + reaction product reactions. This correction,  $F$ , has been described in detail [19, 20] and has the following form:

$$F = \frac{(k_{DMS} - k_P)}{k_{DMS}} \times \frac{1 - \frac{[DMS]_t}{[DMS]_0}}{\left(\frac{[DMS]_t}{[DMS]_0}\right)^{k_P/k_{DMS}} - \frac{[DMS]_t}{[DMS]_0}} \quad \text{II}$$

$k_{DMS}$  is the OH + DMS rate constant, and  $k_P$  is the rate constant for the reaction of OH with reaction product. The measured value for  $k_P$  was used when possible, but  $k_P$  was calculated using SAR [18] when no measured value was available in the literature.  $F$ , the correction factor, was multiplied by the product concentration data to account for OH + product reactions and improve the accuracy of product yield determinations.

### 3.3 Monomethyl Succinate (MMS, $CH_3OC(=O)CH_2CH_2C(=O)OH$ )

Using GC/FID, a peak at retention time = 17.7 min was observed to increase with each exposure to light when performing OH + DMS reaction product experiments. This product was hypothesized to be monomethyl succinate (MMS), which was verified by GC/MS/FTIR. Verification was performed by placing 10 mL of a 10% wt. solution of MMS and water into a 100-L Teflon® bag, heating the bag and chamber to 30°C for 24 hours, and then sampling as described above. A small solitary peak with the same retention time as the product peak observed in the product yield experiments verified MMS identification. The low vapor pressure of MMS made quantification difficult. Instead, the DMS calibration factor multiplied by 0.75 was used to determine MMS yield (three non-carbonyl carbons in MMS compared to four non-carbonyl carbons in DMS, assuming C=O groups do not contribute to the FID signal). With this assumption, a  $2.17 \pm 0.25\%$  MMS yield from OH + DMS reaction was observed. The rate constant for OH + MMS,

$1.95 \times 10^{-12} \text{ cm}^3 \text{ molecule}^{-1} \text{ s}^{-1}$  (calculated using SAR [18]), was used for  $k_p$  in eq. 7 and resulted in an average [MMS] correction of 24% (maximum correction 43%).

Figure 2 is a plot of the loss of parent compound, DMS, against the *corrected* formation of product, MMS. It should be noted that the corrected product yield exhibited a linear concentration profile. The lack of curvature strongly suggests that no unusual side reactions generated or removed the primary reaction product. The reported error in the product yield is the 95% confidence level from the random uncertainty in the slope of this plot.

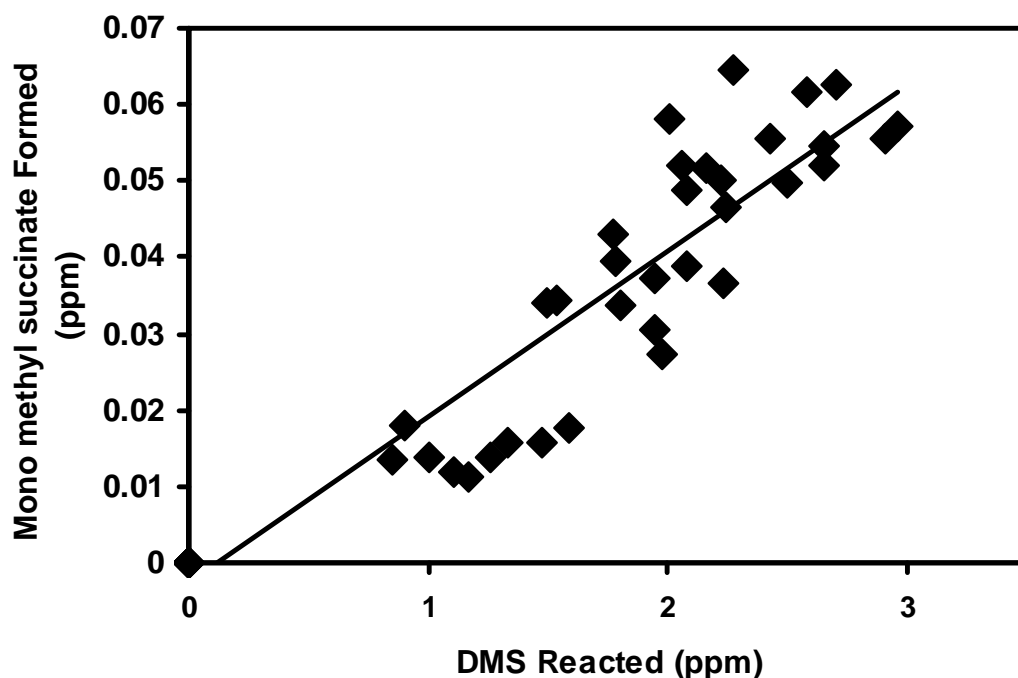


**Figure 2.** Plot of monomethyl succinate formed versus DMS reacted. The slope of the linear least squares analysis with 95% confidence interval is  $0.022 \pm 0.003$ .

The MMS yield was lower than expected since SAR predicts fairly equal hydroxyl radical hydrogen abstraction at the two distinct sites [18]. MMS is highly water soluble and

oxygenated, which could lead to a significant portion of MMS sticking to the chamber walls. To check for MMS wall losses, a typical product yield experiment was performed with a variation in the sampling technique. The chamber was deflated by vacuum until almost empty (the walls did not touch), partly inflated with dry compressed air, and rinsed three times with 50 mL portions of methanol. The rinses were collected in a round-bottom flask, concentrated to 5 mL, and analyzed by liquid injection onto a GC-FID/MS. Traces of MMS and DMS were detected because the chamber was not completely evacuated to prevent the walls from touching, but the results demonstrated no evidence of MMS sticking to the walls nor were other peaks detected.

Product experiments were repeated using GC/MS/FTIR, 2, 4-dinitrophenylhydrazine (DNPH) derivatization (method described in experimental methods), and GC/MS/MS (where samples were directly introduced into the mass spectrometer source). None of these experiments altered the previously observed product yield of MMS.

The apparent “low” MMS yield observed is consistent with previous literature. In the experimental determination of the OH rate constant for dimethyl adipate (DBE-6,  $\text{CH}_3\text{OC}(=\text{O})\text{CH}_2\text{CH}_2\text{CH}_2\text{CH}_2\text{C}(=\text{O})\text{OCH}_3$ ) it was determined that the experimental  $k_{\text{OH}}(\text{DBE-6})$  was two times higher than the calculated  $k_{\text{OH}}(\text{DBE-6})$  using SAR [17]. In this study, the authors hypothesize that the two central  $-\text{CH}_2-$  groups in DBE-6 are “underestimated” by current SAR techniques [17]. They conclude that for C–H bonds  $\beta$  to a carbonyl ( $\text{C}=\text{O}$ ) and to an ester ( $\text{C}(=\text{O})\text{OR}$ ) there is an approximate three-fold enhancement in the OH radical H-atom abstraction. This  $\beta$ -enhancement was not incorporated in the SAR estimation method developed by Kwok and Atkinson [6], but neighboring functional group influence on OH rate constant estimation is now being addressed by the atmospheric

research community. A new SAR calculation incorporating neighboring-group effects by Neeb [21] uses “an extended set of group rate constants.” The results of these new calculations indicate that, overall, only “10% of the molecules show deviations larger than 50%” from experimental values and that “ethers and ketones are in better agreement with experimental data” than with the Kwok and Atkinson SAR calculation [6].

This  $\beta$ -enhancement may therefore also influence the actual products of OH + compound. In a Tuazon *et al* [22] study of OH + dimethyl glutarate (DBE-5,  $\text{CH}_3\text{OC}(=\text{O})\text{CH}_2\text{CH}_2\text{CH}_2\text{C}(=\text{O})\text{OCH}_3$ ), monomethyl glutarate was observed as one of the major products at a yield of  $34 \pm 16\%$ . The formation of monomethyl glutarate is due to H-atom abstraction at the central  $-\text{CH}_2-$ , which happens to be  $\beta$  to two ester groups on either side. With the possibility that there is OH reactivity enhancements at such sites, it can be suggested that the yield of monomethyl glutarate is higher than would be expected from normal SAR calculations, perhaps by a factor of three.

Dimethyl succinate does not have a central  $-\text{CH}_2-$  group that is simply  $\beta$  to an ester group as with DBE-5 and DBE-6, instead the  $-\text{CH}_2-$  groups are on one side  $\beta$  and on the other side  $\alpha$  to an ester group. Therefore the central  $-\text{CH}_2-$  groups in DMS do not see the  $\beta$ -enhancement as do DBE-5 and DBE-6. Without the enhancement reactivity at the central  $-\text{CH}_2-$  groups, and perhaps due to steric hindrance, there is less H-atom abstraction at these two groups compared to DBE-5. Because the mechanism for producing MMS requires abstraction from one of these central  $-\text{CH}_2-$  groups, one would then expect a much lower yield of MMS, perhaps 1/3 less than the  $34 \pm 16\%$  monomethyl glutarate yield from DBE-6. Thus the  $2.17 \pm 0.25\%$  yield of MMS is supported theoretically and experimentally.



### **3.4 Formic Acid (FA, $\text{HOC(=O)H}$ )**

Using a Finnigan Thermoquest GC/Q (MS/MS) and through direct injection of a cryogenically trapped 1.3-mL gas sample, MS analyses were performed on pre-photolyzed and photolyzed chamber contents as described above. Spectral subtraction (photolyzed minus pre-photolyzed) resulted in a large MS ion peak at  $m/z$  46. Further analysis attributed this peak to formic acid (FA).

FA has poor response using FID and it cannot be chromatographed using a Restek RTX-1 column, which was used to determine the OH rate constant for DMS and the product yield of MMS; therefore, a Restek Stabilwax column was placed on a GC/MS and product studies were conducted as described previously. It was observed that FA's concentration was not stable in duplicate runs but always increased for the second sample collection. Experiments were then conducted where the chamber was photolyzed for 60 sec. and then GC/MS samples were collected and analyzed every 30 minutes until FA appeared and stabilized. Each experiment verified that after an induction time, FA was formed, continued to linearly form for a period of time, and then remained constant, all in the dark after an initial 60-second photolysis (Figure 3). The formic acid "yield" was approximately unity as a FA molecule was generated from each DMS molecule consumed. These experiments strongly suggest that formic acid is a secondary product of a significant primary product.

### **3.5 Nitrate/Nitrite Products**

Nitrate/nitrite product formation has been observed previously in the reaction of dimethyl glutarate (DBE-5,  $\text{CH}_3\text{OC(=O)CH}_2\text{CH}_2\text{CH}_2\text{(O=)COCH}_3$ ) and OH [22], thus experiments were conducted to determine possible nitrate/nitrite products from OH + DMS.

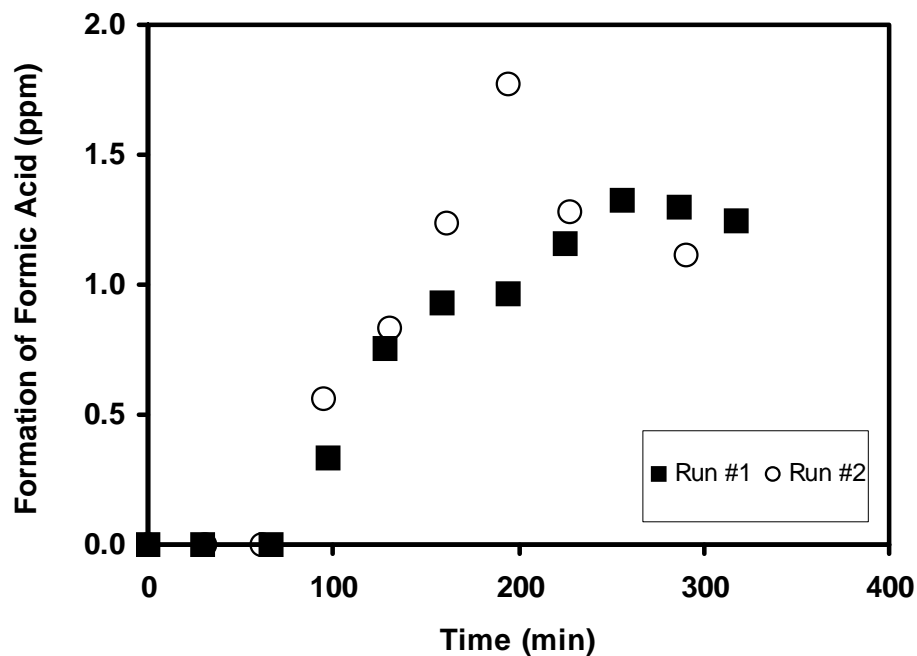
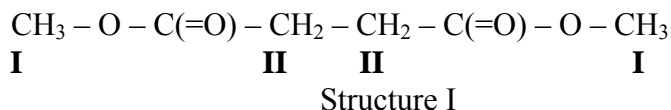


**Figure 3.** Formic acid formation over time after initial 60 second photolysis of 3.0 ppm formic acid, 1.9 ppm nitric oxide, and 40 ppm methyl nitrite.

Excess nitric oxide (NO) and nitrogen dioxide (NO<sub>2</sub>) were added to the chamber (containing DMS, MN, and NO, concentrations mentioned previously) either before or after photolysis. Excess NO and NO<sub>2</sub> should drive the formation of nitrate/nitrite products if the reaction takes place. Methyl nitrite photolysis creates nitrate and nitrite products that are observed by the GC-FID and GC/MS/FTIR systems in our laboratory. However, in these nitrate/nitrite “forcing” experiments, GC-FID experimental results showed no increase in any “new” product peaks. Also, GC/MS/MS showed no indication of additional products.

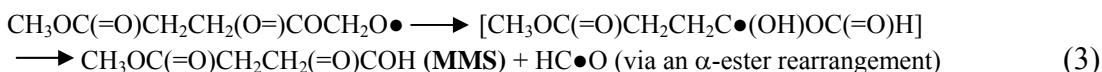
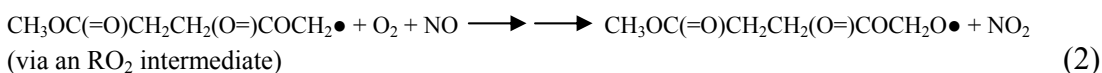
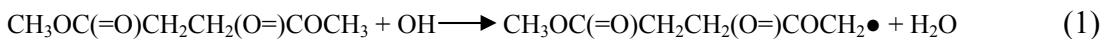
## 4.0 DISCUSSION

OH reacts with dimethyl succinate (DMS) by hydrogen abstraction. DMS is a large symmetrical molecule with two distinct sites for possible H-abstraction.



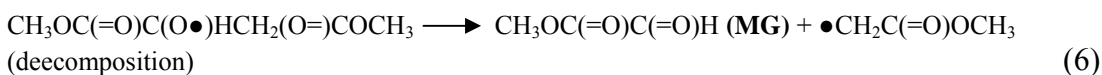
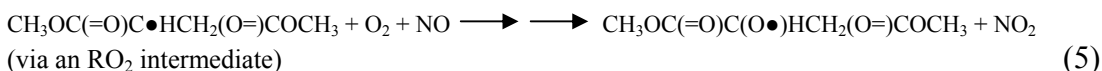
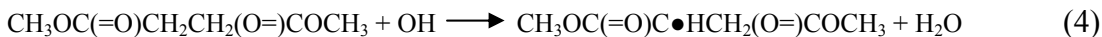
Structure–activity relationships [18] indicate a slight favoring for reaction at site II (SAR for site I =  $0.218 \times 10^{-12} \text{ cm}^3 \text{ molecule}^{-1} \text{ s}^{-1}$  and for site II =  $0.356 \times 10^{-12} \text{ cm}^3 \text{ molecule}^{-1} \text{ s}^{-1}$ ). As opposed to producing large product yields, which would lend evidence to its being the favored site of reaction, it appears that DMS decomposes when attacked at site II. The products produced from reaction at site II appear to be unstable and quickly react to form secondary, small molecules such as formic acid. There is a significantly larger yield for these small molecules from site II than for products from site I, which is evidence for H-abstraction to preferentially take place at site II. This would be consistent with SAR estimates. Despite the uncertainty of the OH reaction mechanism, there is agreement between the SAR calculation ( $1.15 \times 10^{-12} \text{ cm}^3 \text{ molecule}^{-1} \text{ s}^{-1}$ ) and the measured  $k_{DMS}$  ( $1.5 \pm 0.4 \times 10^{-12}$ , this work, and  $1.4 \pm 0.6 \times 10^{-12} \text{ cm}^3 \text{ molecule}^{-1} \text{ s}^{-1}$  [17]).

Depending on the nature of the radical formed by reaction at site I, monomethyl succinate (MMS,  $\text{CH}_3\text{OC}(=\text{O})\text{CH}_2\text{CH}_2(\text{O})\text{COH}$ ) may be formed by  $\alpha$ -ester rearrangement [23]. For reaction site I:

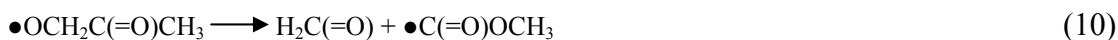
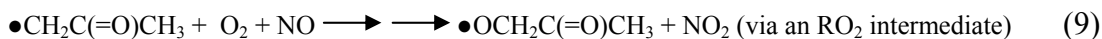


Formic acid (FA, HOC(=O)H) is a secondary product possibly formed via an unstable intermediate. Methyl glyoxylate (MG, CH<sub>3</sub>OC(=O)C(=O)H) is easily polymerized and is not expected to be seen via gas chromatography.

For reaction site II:

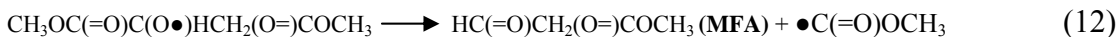


The radical product in Reaction 6 will continue to react:



Formic acid (FA) is produced as a secondary product via an unknown mechanism at this time. The rest of DMS decomposition product (Reactions 9–11) will subsequently produce CO<sub>2</sub> and H<sub>2</sub>CO, neither of which can be monitored due to high background levels and/or their production from the photolysis of methyl nitrite. The slow rise and plateau of FA suggests that there is a limited source of the FA precursor. The fact that the observed [FA] is approximately equivalent to [DMS] lost to reaction with OH also suggests an initial product that breaks down resulting in FA.

Another possible decomposition pathway of Reaction 6 could produce methyl (2-formyl) acetate (MFA,  $\text{HC(=O)CH}_2\text{(O=)COCH}_3$ ):



MFA is similar in structure to ethyl (2-formyl) acetate (EFA,  $\text{HC(=O)CH}_2\text{(O=)COCH}_2\text{CH}_3$ ), a product observed by this laboratory in the study of OH + 3-ethoxypropionate [24]. Therefore if MFA were produced, it should be detected by GC/MS. Close examination of the product data revealed no evidence of the formation of MFA.

The proposed OH + DMS reaction mechanism is shown in Figure 4.

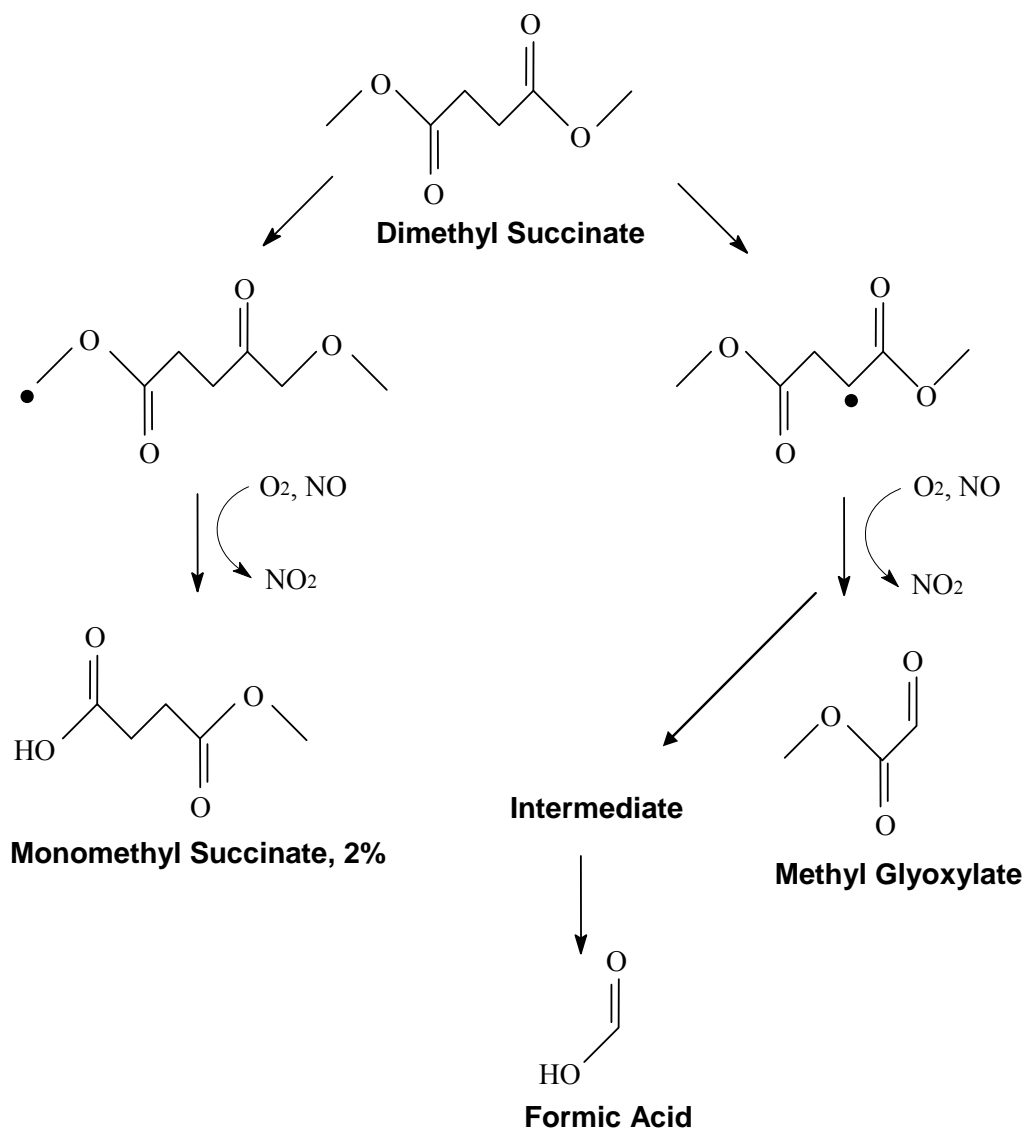


**Figure 4.** Proposed reaction mechanism for hydroxyl radical with dimethyl succinate. Major products are in bold typeface.

### *Acknowledgment*

The authors gratefully thank Dr. Jean Renard for helpful technical discussions.

## 5.0 REFERENCES

1. J.R. Wells, F.L. Wiseman, D.C. Williams, J.S. Baxley, D.F. Smith, *Int. J. Chem. Kinet.*, **28**, 475 (1996).
2. D.F. Smith, C.D. McIver, T.E. Kleindienst, *Int. J. Chem. Kinet.*, **27**, 453 (1995).
3. D.F. Smith, T.E. Kleindienst, E.E. Hudgens, C.D. McIver, J.J. Bufalini, *Int. J. Chem. Kinet.*, **24**, 199 (1992).
4. T.J. Wallington, J.M. Andino, A.R. Potts, S.J. Rudy, W.O. Siegl, Z. Zhang, M.J. Kurylo, R.E. Huie, *Environ. Sci. Technol.*, **27**, 98 (1993).
5. M. Veillerot, P. Foster, R. Guillermo, J.C. Galloo, *Int. J. Chem. Kinet.* **28**, 235 (1996).
6. E.S.C. Kwok, R. Atkinson, *Atmos. Environ.*, **29**, 1685 (1995).
7. W.P.L. Carter, *J. Air and Waste Man. Assoc.*, **44**, 881 (1994).
8. J.H. Seinfeld, *Science*, **243**, 745 (1989).
9. M.S. Bergin, A.G. Russell, J.B. Milford, *Environ. Sci. Technol.* **1998**, 32, 694.
10. R. Atkinson, W.P.L. Carter, A.M. Winer, J.N. Pitts, Jr., *J. Air Pol. Control*, **31**, 1090 (1981).
11. L.N. O'rji and D.A. Stone, *Int. J. Chem Kinet.*, **24**, 703 (1992).
12. D.C. Williams, L.N. O'rji, D.A. Stone, *Int. J. Chem. Kinet.*, **25**, 539 (1993).
13. D.F. Smith, T.E. Kleindienst, E.E. Hudgens, J.J. Bufalini, *Intern J. Environ. Anal. Chem.*, **54**, 265 (1994).
14. D.F. Smith, T.E. Kleindienst, E.E. Hudgens, *J. Chromatog.*, **483**, 431 (1989).
15. W.D. Taylor, D. Allston, M.J. Moscato, G.D. Fazekas, R. Kozlowski, G.A. Takacs, *Int. J. Chem. Kinet.*, **12**, 231 (1980).
16. R. Atkinson, *J. Phys. Chem. Ref Data*, Monograph No. 2, (1994).
17. S. Aschmann, R. Atkinson, *Int. J. Chem. Kinet.*, **30**, 471–474 (1998).
18. AOPWIN v1.89, SRC-AOP for Microsoft Windows, Copyright © William Meylan, 1994–1999.
19. D.F. Smith, C.D. McIver, T.E. Kleindienst, *Int. J. Chem. Kinet.*, **27**, 453 (1995).

20. R. Atkinson, S.M. Aschmann, W.P.L. Carter, A.M. Winer, and J.N. Pitts, Jr., *J. Phys. Chem.*, **86**, 4563 (1982).
21. P. Neeb, *J. Atmos. Chem.*, **35**, 295 (2000).
22. E. C. Tuazon, S. M. Aschmann, and R. Atkinson, *Env. Sci. and Tech.*, **33**, 2885 (1999).
23. E. C. Tuazon, S. M. Aschmann, R. Atkinson, and W. Carter, *J. Phys. Chem. A*, **102**, 2316–2321 (1998).
24. S. Baxley, M. Henley, J.R. Wells, *Int. J. Chem. Kinet.*, **29**, 637–644 (1997).